

Eddy-Current-Induced Multipole Field Calculations

Nicholas S. Sereno, Suk H. Kim

1.0 Abstract

Time-varying magnetic fields of magnets in booster accelerators induce substantial eddy currents in the vacuum chambers. The eddy currents in turn act to produce various multipole fields that act on the beam. These fields must be taken into account when doing a lattice design. In the APS booster, the relatively long dipole magnets (3 meters) are linearly ramped to accelerate the injected 325 MeV beam to 7 GeV. Substantial dipole and sextupole fields are generated in the elliptical vacuum chamber from the induced eddy currents. In this note, formulas for the induced dipole and sextupole fields are derived for elliptical and rectangular vacuum chambers for a time-varying dipole field. A discussion is given on how to generalize this derivation method to include eddy-current-induced multipole fields from higher multipole magnets (quadrupole, sextupole, etc.). Finally, transient effects are considered.

2.0 Calculation of Eddy-Current-Induced Dipole and Sextupole Fields

In this section we derive general formulas for the induced dipole and sextupole fields for a time-varying, but otherwise constant, dipole field along the y axis $\vec{B} = B_y \hat{y} = B_o(t) \hat{y}$.

From Faraday's law, this field generates a longitudinal electric field where we ignore any longitudinal dependence on the fields (ignore end effects). After integration, the longitudinal electric field is given by $\vec{E} = E_z(x) \hat{z} = x \frac{dB_o}{dt} \hat{z}$ in mks units. This electric field will

set up eddy currents in any conducting vacuum chamber present. Figure 1 shows the coordinate system used to evaluate the effect of the induced currents.

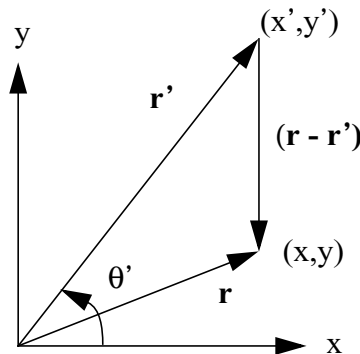


Figure 1: Source and field-point geometry for eddy-current calculation.

In the figure, the field point is denoted by the vector \mathbf{r} and coordinates (x,y). The source point is denoted by the vector \mathbf{r}' at angle θ' and coordinates (x',y'). Using these coordinates and the Biot-Savart law,

$$d\vec{B}(\vec{r}) = \left(\frac{\mu_o}{4\pi}\right) \frac{I(\vec{r}') d\vec{l} \times (\vec{r} - \vec{r}')}{(\vec{r} - \vec{r}')^3}, \quad 2.1$$

the total magnetic field at any point \mathbf{r} is obtained by integrating over the volume containing the eddy currents (i.e., the volume of the vacuum chamber cross section). The current element is along z and is given in terms of the longitudinal electric field by Ohm's law:

$$I(\vec{r}') d\vec{l} = j_z(x', y') dx' dy' dz' \hat{z} = \sigma E_z(x) dx' dy' dz' \hat{z} = x \frac{dB_o}{dt} \sigma dx' dy' dz' \hat{z}, \quad 2.2$$

where σ is the conductivity of the vacuum chamber. Using this equation, equation 2.1 becomes a volume integral for the magnetic field:

$$\vec{B}(\vec{r}) = \int_V \left(\frac{\mu_o}{4\pi}\right) \frac{j_z(x', y') \hat{z} \times (\vec{r} - \vec{r}')}{(\vec{r} - \vec{r}')^3} dx' dy' dz'. \quad 2.3$$

This equation can be simplified by integrating over z ($-\infty < z < \infty$), thereby ignoring end effects. Finally, converting to cylindrical coordinates the Biot-Savart law becomes:

$$B_x(x, y) = \left(-\frac{\mu_o \sigma}{2\pi}\right) \frac{dB_o}{dt} \int \frac{r'^2 \cos \theta' (y - r' \sin \theta')}{(x - r' \cos \theta')^2 + (y - r' \sin \theta')^2} dr' d\theta' \quad 2.4$$

$$B_y(x, y) = \left(\frac{\mu_o \sigma}{2\pi}\right) \frac{dB_o}{dt} \int \frac{r'^2 \cos \theta' (x - r' \cos \theta')}{(x - r' \cos \theta')^2 + (y - r' \sin \theta')^2} dr' d\theta', \quad 2.5$$

where the integration is taken over the cross-sectional area of the vacuum chamber where eddy currents exist. The last two equations can be used to determine the field at any point for a vacuum chamber of arbitrary cross section.

This derivation is implicitly not self-consistent due to the fact that the eddy-current distribution also depends on its own rate of change. Dropping self-consistency is not a bad assumption since the time rate of change of the eddy currents is actually proportional to the second time derivative of the main driving field (in this note a driving dipole field). For the APS booster, this second derivative is exactly zero since the booster has a linear ramped field when beam is in the machine. For resonant boosters, the second time derivative of the driving field is only substantial when the first derivative of the field changes

sign (when the actual drive field is maximum or minimum). The beam is usually not in the machine at the maximum or minimum points in the booster cycle.

3.0 General Derivation of Eddy-Current-Induced Multipole Strength Parameters

From the eddy-current-induced fields derived in the last section, we can easily derive the multipole strength parameters by expanding the integrands and identifying the multipole terms. Alternatively, the strength parameters are given as straightforward derivatives of the vertical component of the field with respect to x evaluated at the field point $x = y = 0$ [1]:

$$s_n(m^{-n}) = \left. \frac{e}{cp} \frac{\partial^{(n-1)} B_y}{\partial x^{(n-1)}} \right|_{x=y=0}, \quad 3.1$$

where n is the order of the multipole ($n=1$ =dipole, $n=2$ =quadrupole, $n=3$ =sextupole, etc.). Performing the differentiation using the integral equation for the vertical field component given by equation 2.5 yields:

$$s_1(m^{-1}) = \kappa_x = \rho^{-1} = \left(-\frac{e}{cp} \right) \left(\frac{\mu_o \sigma}{2\pi} \right) \frac{dB_o}{dt} \int r' (\cos \theta')^2 dr' d\theta' \quad 3.2$$

$$s_2(m^{-2}) = k = \left(-\frac{e}{cp} \right) \left(\frac{\mu_o \sigma}{2\pi} \right) \frac{dB_o}{dt} \int \cos \theta' \sin 2\theta' dr' d\theta' \quad 3.3$$

$$s_3(m^{-3}) = m = \left(\frac{e}{cp} \right) \left(\frac{\mu_o \sigma}{2\pi} \right) \frac{dB_o}{dt} \int \frac{2(\cos \theta')^2 (3 - 4(\cos \theta')^2)}{r'} dr' d\theta', \quad 3.4$$

for the first three multipoles. In general, the lowest order multipoles will have the highest influence on the beam. The multipoles will also be important for a machine like the APS booster at low energy, where the strength parameters are maximum.

4.0 Multipole Strengths for Elliptical and Rectangular Vacuum Chamber Cross Sections

Figures 2 and 3 show the eddy-current source and field-point geometries for the elliptical and rectangular chambers. The region of integration is defined by the inner and outer elliptical surfaces. The integrals given by equations 3.2 to 3.4 are most conveniently evaluated by first integrating the radial vector between the limits defined by the geometry of the

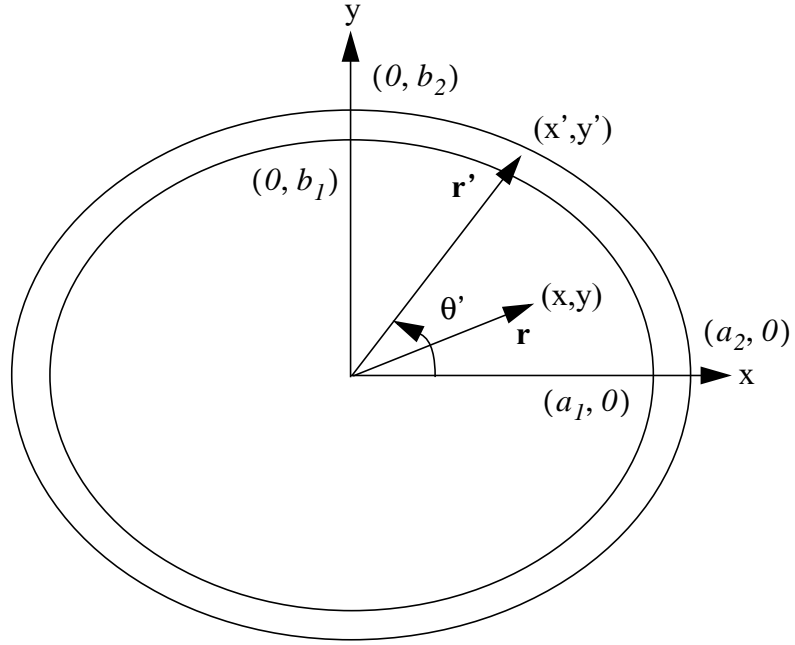


Figure 2: Source and field-point geometry for the elliptical chamber.

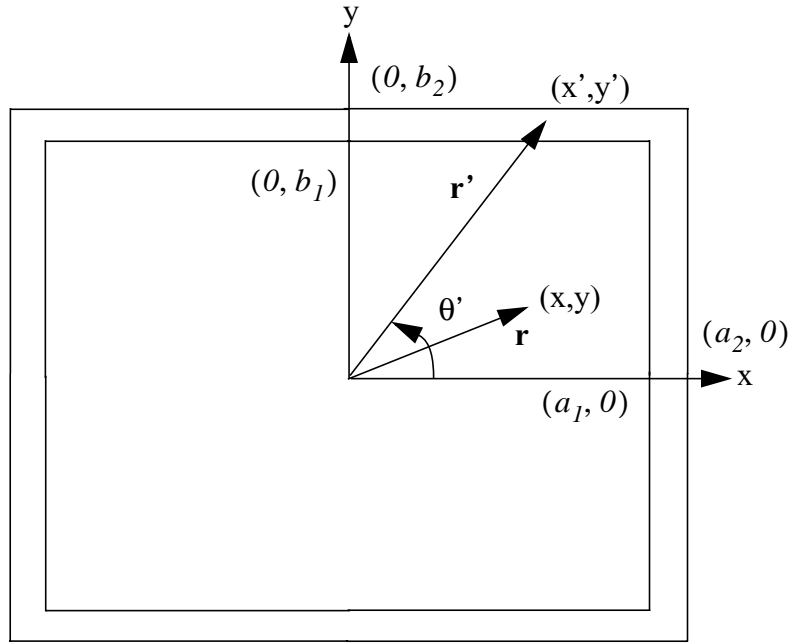


Figure 3: Source and field-point geometry for the rectangular chamber.

inner and outer surfaces and then integrating over angle. For the elliptical chamber, these limits are specified by:

$$r'_{I(2)} = \left(\frac{I}{\sqrt{\left(\frac{\cos \theta'}{a_{I(2)}}\right)^2 + \left(\frac{\sin \theta'}{b_{I(2)}}\right)^2}} \right); \quad (0 \leq \theta' \leq 2\pi), \quad 4.1$$

where $r'_{I(2)}$ define the inner and outer elliptical surfaces of the vacuum chamber. The rectangular limits of integration are more complex, and the integration must be done piecewise (rectangular coordinates would be more convenient to use):

$$\begin{aligned} r'_{I(2)} &= \frac{a_{I(2)}}{\cos \theta'}; \quad 0 \leq \theta' \leq \theta'_1 = \text{atan}\left(\frac{b_1}{a_1}\right) \\ r_1 &= \frac{b_1}{\sin \theta'}; \quad r_2 = \frac{a_2}{\cos \theta'}; \quad \theta'_1 \leq \theta' \leq \theta'_2 = \text{atan}\left(\frac{b_2}{a_2}\right) \\ r_{I(2)} &= \frac{b_{I(2)}}{\sin \theta'}; \quad \theta'_2 \leq \theta' \leq \pi - \theta'_2 \\ r_1 &= \frac{b_1}{\sin \theta'}; \quad r_2 = \frac{-a_2}{\cos \theta'}; \quad \pi - \theta'_2 \leq \theta' \leq \pi - \theta'_1 \\ r'_{I(2)} &= \frac{-a_{I(2)}}{\cos \theta'}; \quad \pi - \theta'_1 \leq \theta' \leq \pi, \end{aligned} \quad 4.2$$

where the total integral is twice the sum of the integrals defined by these limits (by symmetry). The calculation of the strength parameters was tedious and extensive use was made of Mathematica [2].

4.1 Strength Parameters for the Elliptical Chamber

For these chamber geometries, the quadrupole strength parameter $s_2(m^{-2}) = k = 0$, by symmetry. Only for a nonsymmetric chamber is there an induced quadrupole field. For the elliptical chamber, the result for the dipole and sextupole strengths is:

$$\begin{aligned} \frac{s_1(m^{-1})}{\left(-\frac{e}{cp}\right)\left(\frac{\mu_o \sigma}{2\pi}\right)\frac{dB_o}{dt}} &= \pi \left(\frac{a_2^2 b_2}{a_2 + b_2} - \frac{a_1^2 b_1}{a_1 + b_1} \right) \\ &= \pi t \left(\frac{(\epsilon^3 + 4\epsilon^2 + 7\epsilon + 4)b_2^2 - (2\epsilon^2 + 7\epsilon + 6)b_2 t + (\epsilon + 2)t^2}{(\epsilon + 2)((\epsilon + 2)b_2 - 2t)} \right) \end{aligned} \quad 4.11$$

$$\begin{aligned} \frac{s_3(m^{-3})}{\left(\frac{e}{cp}\right)\left(\frac{\mu_o\sigma}{2\pi}\right)\frac{dB_o}{dt}} &= 2\pi\left(\frac{a_1^2b_2(2a_2+b_2)-a_2^2b_1^2-2a_1a_2^2b_1}{(a_1+b_1)^2(a_2+b_2)^2}\right) \\ &= 2\pi\epsilon t\left(\frac{2(\epsilon^2+3\epsilon+2)b_2-(3\epsilon+4)t}{(\epsilon+2)^2((\epsilon+2)b_2-2t)^2}\right), \end{aligned} \quad 4.12$$

where $t \equiv a_2 - a_1 = b_2 - b_1$ is the vacuum chamber thickness and $\epsilon \equiv \frac{a_2 - b_2}{b_2}$ is a measure of the elliptical shape of the chamber. For the case $t \ll a_{1(2)}$; $t \ll b_{1(2)}$ and $\epsilon \ll 1$, the previous formulas can be expanded in powers of the small parameters:

$$\frac{s_1(m^{-1})}{\left(-\frac{e}{cp}\right)\left(\frac{\mu_o\sigma}{2\pi}\right)\frac{dB_o}{dt}} = \pi b_2 t \left(1 - \frac{t}{2b_2} + \frac{3}{4}\epsilon + \frac{\epsilon^3}{16} + \dots\right) \quad 4.13$$

$$\frac{s_3(m^{-3})}{\left(\frac{e}{cp}\right)\left(\frac{\mu_o\sigma}{2\pi}\right)\frac{dB_o}{dt}} = \frac{\pi}{2}\left(\frac{\epsilon t}{b_2}\right)\left(1 - \frac{\epsilon}{2} + \frac{t}{b_2} - \frac{3}{4}\left(\frac{\epsilon t}{b_2}\right) + \frac{t^2}{b_2^2} + \dots\right), \quad 4.14$$

where the formulas are to 4th order in the product ϵt . The sextupole strength given by equation 4.14 agrees with the equation listed in reference [3].

4.2 Strength Parameters for the Rectangular Chamber

Once again, for the rectangular chamber case, the only parameters that are nonzero are the dipole and sextupole strengths. After performing the piecewise integration, the dipole and sextupole formulas are given by:

$$\frac{s_1(m^{-1})}{\left(-\frac{e}{cp}\right)\left(\frac{\mu_o\sigma}{2\pi}\right)\frac{dB_o}{dt}} = \pi(b_2^2 - b_1^2) + 2(a_1b_1 - a_2b_2) + \quad 4.21$$

$$2((a_1^2 + b_1^2)\theta_1' - (a_2^2 + b_2^2)\theta_2') = -t(2(\epsilon + 2 - \pi)b_2 + (\pi - 2)t)$$

$$-2b_2^2(\epsilon^2 + 2\epsilon + 2)(\theta_2' - \theta_1') - 4t((\epsilon + 2)b_2 + t)\theta_1'$$

$$\begin{aligned}
\frac{s_3(m^{-3})}{\left(\frac{e}{cp}\right)\left(\frac{\mu_o \sigma B_o \dot{(t)}}{2\pi}\right)} &= 4 \left(\frac{a_2 b_2}{a_2^2 + b_2^2} - \frac{a_1 b_1}{a_1^2 + b_1^2} + \theta_2' - \theta_1' \right) \\
&= \frac{4\varepsilon^2 t((\varepsilon + 2)b_2 - t)}{((\varepsilon + 2)\varepsilon + 2)((\varepsilon + 2)\varepsilon + 2)b_2^2 - 2b_2 t(\varepsilon + 2) + 2t^2} \\
&\quad + 4(\theta_2' - \theta_1'),
\end{aligned} \tag{4.22}$$

where the parameters t and ε have the same definition in terms of a_1, a_2, b_1 and b_2 as described for the elliptical chamber. Finally, the dipole and sextupole strength parameters can be expressed to 4th order in the product εt as with the elliptical chamber.

$$\frac{s_I(m^{-I})}{\left(-\frac{e}{cp}\right)\left(\frac{\mu_o \sigma B_o \dot{(t)}}{2\pi}\right)} = t b_2 \left(4 + \pi \varepsilon + \frac{\varepsilon^3}{3} - \frac{2t}{b_2} + \dots \right) \tag{4.23}$$

$$\frac{s_3(m^{-3})}{\left(\frac{e}{cp}\right)\left(\frac{\mu_o \sigma B_o \dot{(t)}}{2\pi}\right)} = \frac{2\varepsilon t}{b_2} \left(1 + \frac{t}{b_2} + \frac{t^2}{b_2^2} - \varepsilon^2 + \dots \right). \tag{4.24}$$

5.0 Eddy-Current-Induced Multipoles for Quadrupole and Sextupole Fields

The method presented in section 2.0 can be generalized to describe the effect of time-varying (upright) quadrupole and sextupole (and higher) multipole fields. Here we concentrate on quadrupole and sextupole fields, since these will be the most important. The main difference between these multipoles and the dipole field is that the induced longitudinal electric field now has both x and y dependence. The result for the electric field for the quadrupole is [1]:

$$E_z(x, y) = \frac{\dot{g}}{2}(x^2 - y^2), \tag{5.1}$$

and for the sextupole is:

$$E_z(x, y) = \frac{\dot{s}x}{2} \left(\frac{x^2}{3} - y^2 \right), \tag{5.2}$$

where Faraday's law was used to obtain the longitudinal electric field as with the dipole. Here the time derivative of the quadrupole gradient and sextupole gradient are represented by the dot. Ohm's Law and the Biot-Savart law are then used with these expressions to derive the eddy-current-induced magnetic field distribution in the vacuum chamber. The multipole strength parameters are obtained using equation 3.1 as before. It is best to integrate the nontrivial integrals numerically over the cross section of the vacuum chamber to determine the strength parameter. Finally, multipole fields induced by eddy currents generated by time-varying skew multipoles can be calculated using the method presented in this note.

6.0 Transient Considerations

In this section we consider transient effects for the case of a time varying dipole field $B_y(t)$. As with the calculation of the induced multipole strength, end effects are neglected and the eddy currents flow in the longitudinal (z) direction. The eddy current due to the inducing field $B_y(t')$ at a time t' acts to reduce the total field inside the vacuum chamber at the present time t where $t > t'$. The eddy currents decay with time constant τ . The field inside the chamber at time t , $B_i(t)$ can be calculated by subtracting the eddy current induced field from the main field [4]:

$$B_i(t) = B_y(t) - \int_0^t \frac{\partial}{\partial t} B_y(t-t') e^{-\frac{t'}{\tau}} dt' = \frac{I}{\tau} \int_0^t B_y(t-t') e^{-\frac{t'}{\tau}} dt' \quad 6.1$$

after integration by parts. Equation 6.1 expresses the fact that the eddy currents (proportional to the time derivative of the inducing field $B_y(t')$) decay away with time constant τ . The net effect on the field inside the chamber is found by adding up (integrating) for all times t' prior to the present time t .

Since $B_y(t-t') = 0$, $t \leq t'$, the convolution theorem of the Laplace transform applied to equation 6.1 yields:

$$B_i(s) = \frac{B_y(s)}{I + s\tau}, \quad 6.2$$

where s is the Laplace variable. Equation 6.2 is of course equivalent to equation 6.1 and may be more convenient for arbitrary $B_y(t')$. For example, the time constant for the APS booster stainless-steel vacuum chamber is approximately 1 ms. For a 1 ms time constant, the field inside the chamber is reproduced to less than 1%. There is also a phase shift introduced in the waveform. This phase shift is mainly due to the fact that the eddy currents are proportional to the derivative of the inducing field as shown in equation 6.1. The time constant τ is simply proportional to the conductivity and the thickness of the vacuum chamber material as given by the formula in reference [3].

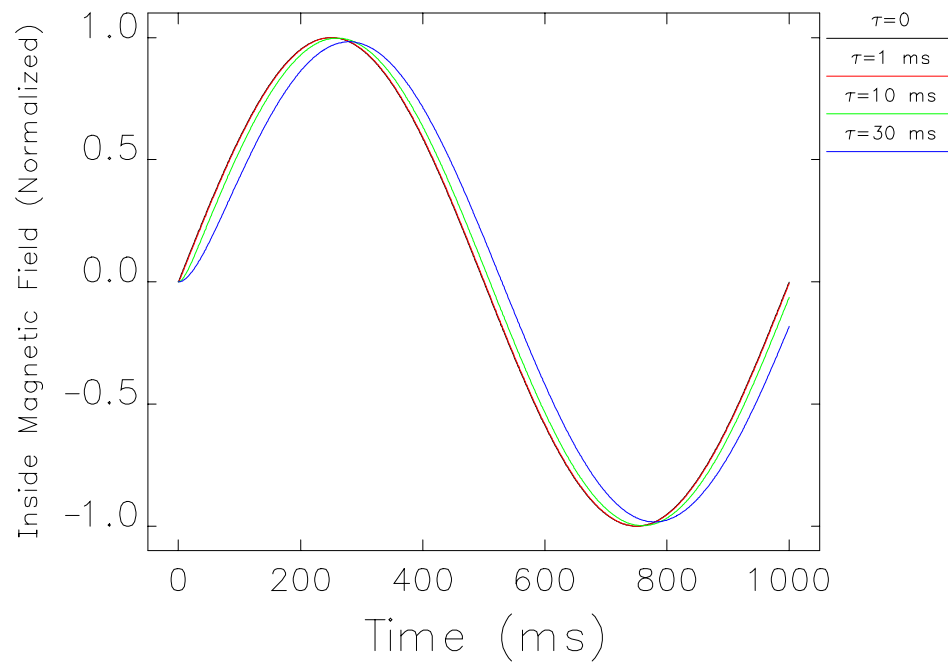


Figure 4: Magnetic field inside the vacuum chamber for four different values of the time constant. The drive field is sinusoidal.

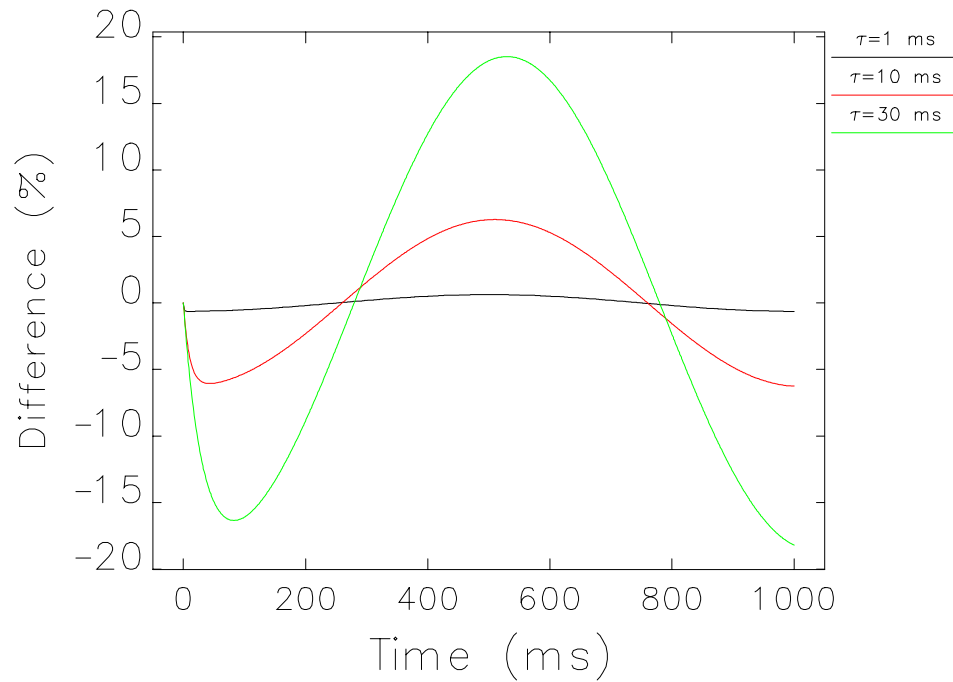


Figure 5: Difference between the magnetic field inside the chamber and drive field ($\tau=0$ ms) in percent. One sees the transient effect starts to become substantial at $\tau \sim 10$ ms.

Figure 4 shows the magnetic field inside the chamber for four different values of the time constant τ for a sinusoidal drive field. This drive field is a good approximation to the APS booster field when the beam is in the machine. When the value of the time constant is 0, the drive field is reproduced, which in this case is a sinusoid. As the time constant is increased, the amplitude and phase of the waveforms change. Figure 5 shows the difference between the curves with nonzero τ and the main drive field ($\tau=0$). For large time constants, one would have to tailor the drive field to get the actual field profile desired. For the APS booster, transient effects are seen to be small, and the net effect is a slight reduction in the field the beam actually sees.

7.0 Acknowledgments

The authors would like to thank Glenn Decker, Louis Emery, Lee Teng for many useful comments and suggestions. Thanks to Lee Teng for pointing out the self-consistency assumption implicit in the derivation.

8.0 References

- [1] H. Wiedemann, *Particle Accelerator Physics: Basic Principles and Linear Beam Dynamics*, Springer-Verlag, pp. 94-95, 1993.
- [2] S. Wolfram, “*Mathematica: A System for Doing Mathematics by Computer*,” Version 4.2.1.0, License ID: L2129-0917, 1988-2002.
- [3] A. W. Chao, M. Tigner, “*Handbook of Accelerator Physics and Engineering*,” World Scientific, pp. 264, 1999.
- [4] W. R. Smythe, “*Static and Dynamic Electricity*,” McGraw-Hill, New York, 2nd Ed., p. 411, (1950).